Advances in Nano Research, *Vol. 8, No. 4 (2020) 283-292*
DOI: https://doi.org/10.12989/anr.2020.8.4.283

Scale-dependent thermal vibration analysis of FG beams having porosities based on DQM

Raad M. Fenjan, Nader M. Moustafa and Nadhim M. Faleh*

Al-Mustansiriah University, Engineering Collage P.O. Box 46049, Bab-Muadum, Baghdad 10001, Iraq

(*Received November 3, 2019, Revised April 23, 2020, Accepted May 1, 2020*)

Abstract. In the present research, differential quadrature (DQ) method has been utilized for investigating free vibrations of porous functionally graded (FG) micro/nano beams in thermal environments. The exact location of neutral axis in FG material has been assumed where the material properties are described via porosity-dependent power-law functions. A scale factor related to couple stresses has been employed for describing size effect. The formulation of scale-dependent beam has been presented based upon a refined beam theory needless of shear correction factors. The governing equations and the associated boundary conditions have been established via Hamilton's rule and then they are solved implementing DQ method. Several graphs are provided which emphasis on the role of porosity dispersion type, porosity volume, temperature variation, scale factor and FG material index on free vibrational behavior of small scale beams.

Keywords: free vibrations; thermal effects; porosity; FG beam; modified couple stress theory

1. Introduction

Within a FG material, all material properties may change from one side to another side by means of a prescribed distribution (Mahesh *et al*. 2018, 2019, Mahesh and Kattimani 2019, Vinyas and Kattimani 2017a, b, 2018, Vinyas *et al*. 2019a, b, 2020, Vinyas 2020a, b). These two sides may be ceramic or metal. Mechanical characteristics of a FG material can be described based on the percentages of ceramic and metal phases. The material distribution in FG materials may be characterized via a power-law function. FG materials are not always perfect because of porosity production in them. Existence of porosities in the FG materials may significantly change their mechanical characteristics. For example, the elastic moduli of porous FG material is smaller than that of perfect FG material. Up to now, many authors focused on wave propagation, vibration and buckling analyzes of FG structures having porosities (Şimşek and Kocatürk 2009, Hadji *et al*. 2016, Benadouda *et al*. 2017, Belabed *et al*. 2018, Ayache *et al*. 2018, Mahmoudi *et al*. 2018, Safa *et al*. 2019, Zouatnia and Hadji 2019, Wattanasakulpong and Ungbhakorn 2014). Also, there are several investigations concerning with the analysis of FG structures in thermal environments.

Recently, this kind of materials have found their applications in micro-scale structures. Vibration behavior of a micro-scale beam is not the same as a macro-scale beam. This is because small-size effects are not present at macro scale. So, mathematical modeling of a micro-beams can be done with the use of nonlocal elasticity and modified couple stress theory (Yang *et al*. 2002) incorporating only one scale parameter. Due to the ignorance of strain gradient effect in nonlocal elasticity theory, a more general theory will be required. Strain gradients at nano-scale are observed by many researchers. While, couple stresses play a major role in mechanical analysis microsize structures. The scale parameters used in nonlocal and modified couple stress theories can be obtained by fitting obtained theoretical results with available experimental data and even molecular dynamic (MD) simulations (Lu *et al*. 2009, Şimşek and Reddy 2013, Wang and Wang 2011, Liu *et al*. 2013, Akgöz and Civalek 2014, Al-Basyouni *et al*. 2015, Fernández-Sáez *et al*. 2016, Civalek and Demir 2016, Ahmed *et al*. 2019, Attia and Rahman 2018, Barretta *et al*. 2018, Bensattalah *et al*. 2019).

This paper uses a higher order shear deformation beam formulation having three variables without using of shear correction factor. Based upon differential quadrature (DQ) approach and modified couple stress elasticity formulation, mechanical-thermal vibrational analysis of shear deformable porous functionally graded (FG) microbeam has been performed. The presented formulation incorporates one scale factor for examining vibrational behaviors of micro-dimension beams more accurately. The material properties for FG beam are porosity-dependent and defined employing a modified power-law form. It is supposed that the micro-sized beam is exposed to thermal loading of uniform type. The governing equations achieved by Hamilton's principle are solved implementing DQM. Presented results indicate the prominence of temperature variation, scale factor, material gradient index, and porosities on vibrational frequencies of FG micro-size beam.

*Corresponding author, Ph.D., Professor,
E-mail: dr.nadhim@uomustansiriyah.edu.iq;
drnadhim@gmail.com

ISSN: 2287-237X (Print), 2287-2388 (Online)

2. Theoretical formulation

For the micro-size beam shown in Fig. 1, the material distribution in FG materials may be characterized via a power-law function. FG materials are not always perfect because of porosity production in them. Existence of porosities in the FG materials may significantly change their mechanical characteristics. Porosities within the material structure can affect all material properties of FGMs. It is well-known that porosity volume fraction (α), can be incorporated in the rule of mixture to define the material properties of FGMs. Based on the rule of mixture, the effective material properties, P_f, can be expressed by (She *et al*. 2018)

$$P_f = P_c(V_c - \frac{\alpha}{2}) + P_m(V_m - \frac{\alpha}{2}) \tag{1}$$

for which P_c, P_m, V_c and V_m define the material properties and the volume fractions of the metallic and ceramic ingredients, respectively which are related by (She *et al*. 2019)

$$V_c + V_m = 1 \tag{2}$$

By defining the location of neutral axis (z_{ns}) which is different from mid-axis location (z_{ms}), the volume fraction of ceramic ingredient may be introduced by

$$V_c = \left(\frac{z_{ms}}{h} + \frac{1}{2}\right)^p = \left(\frac{z_{ns} + C}{h} + \frac{1}{2}\right)^p \tag{3}$$

in which based on Láme's constants (λ and μ), one may define

$$C = \frac{\int_{-\frac{h}{2}}^{\frac{h}{2}} [\lambda(z_{ms}) + 2\mu(z_{ms})] z_{ms} dz_{ms}}{\int_{-\frac{h}{2}}^{\frac{h}{2}} [\lambda(z_{ms}) + 2\mu(z_{ms})]\, dz_{ms}} \tag{4}$$

In this study, it is assumed that the porosities have even distribution. Also, due to the fact that the microbeam has planar deformation, porosity distribution will be symmetric. Depending on the type of porosity distribution, the elastic moduli E, density ρ, temperature expansion property γ and thermal coefficient k for porous FG material can be expressed in the following power-law form having material gradient index p as

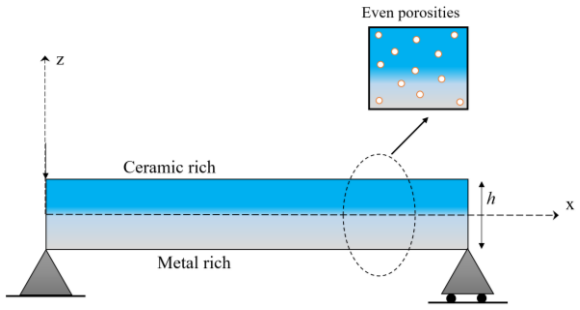

Fig. 1 Geometry of porous beam

$$E(z_{ns}) = (E_c - E_m)\left(\frac{z_{ns} + C}{h} + \frac{1}{2}\right)^p + E_m - (E_c + E_m)\frac{\alpha}{2} \tag{5}$$

$$\rho(z_{ns}) = (\rho_c - \rho_m)\left(\frac{z_{ns} + C}{h} + \frac{1}{2}\right)^p + \rho_m - (\rho_c + \rho_m)\frac{\alpha}{2} \tag{6}$$

$$\nu(z_{ns}) = (\nu_c - \nu_m)\left(\frac{z_{ns} + C}{h} + \frac{1}{2}\right)^p + \nu_m - (\nu_c + \nu_m)\frac{\alpha}{2} \tag{7}$$

$$\gamma(z_{ns}) = (\gamma_c - \gamma_m)\left(\frac{z_{ns} + C}{h} + \frac{1}{2}\right)^p + \gamma_m - (\gamma_c + \gamma_m)\frac{\alpha}{2} \tag{8}$$

$$k(z_{ns}) = (k_c - k_m)\left(\frac{z_{ns} + C}{h} + \frac{1}{2}\right)^p + k_m - (k_c + k_m)\frac{\alpha}{2} \tag{9}$$

where m and c correspond to the metallic and ceramic sides, respectively; α defines the porosity volume fraction. Furthermore, the temperature-dependency of material coefficients might be introduced with usage of the below relation

$$P = P_0(P_{-1}T^{-1} + 1 + P_1T + P_2T^2 + P_3T^3) \tag{10}$$

where P_0, P_1, P_2 and P_3 are material coefficients which can be seen in the Table 1 for SUS304 and Si_3N_4. The bottom surface of FGM beam is pure metal (SUS304), whereas the top surface is pure ceramic (Si_3N_4).

3. The modified couple stress theory

Based upon to the modified couple stress elasticity, the strain energy, U of an elastic material occupying region Ω is associated with the strain and curvature tensors as

$$U = \frac{1}{2}\int_{\Omega} (\sigma_{ij}\varepsilon_{ij} + m_{ij}\chi_{ij})dV \quad (i,j = 1,2,3) \tag{1}$$

where σ, ε, m and χ are Cauchy stress tensor, classical strain tensor, deviatoric part of the couple stress tensor and symmetric curvature tensor, respectively. The strain and curvature tensors can be defined by

$$\varepsilon_{ij} = \frac{1}{2}(u_{i.j} + u_{j.i}) \tag{12}$$

$$\chi_{ij} = \frac{1}{2}(\theta_{i.j} + \theta_{j.i}) \tag{13}$$

where $u_{i.j}$ and $\theta_{i.j}$ are the components of the displacement and rotation vectors written by

Table 1 Material factors of Si_3N_4 and SUS304

Material	Properties	P_0	P_{-1}	P_1	P_2	P_3
Si_3N_4	E (Pa)	348.43e+9	0	-3.070e-4	2.160e-7	-8.946e-11
	γ (K^{-1})	5.8723e-6	0	9.095e-4	0	0
	ρ (Kg/m^3)	2370	0	0	0	0
	κ (W/mK)	13.723	0	-1.032e-3	5.466e-7	-7.876e-11
	ν	0.24	0	0	0	0
SUS304	E (Pa)	201.04e+9	0	3.079e-4	-6.534e-7	0
	γ (K^{-1})	12.330e-6	0	8.086e-4	0	0
	ρ (Kg/m^3)	8166	0	0	0	0
	κ (W/mK)	15.379	0	-1.264e-3	2.092e-6	-7.223e-10
	ν	0.3262	0	-2.002e-4	3.797e-7	0

$$\theta_i = \frac{1}{2} e_{ijk} u_{k.j} \tag{14}$$

in which e_{ijk} is the permutation symbol. The constitutive relations can be expressed as

$$\sigma_{ij} = \lambda(z_{ns})\epsilon_{kk}\delta_{ij} + 2\mu(z_{ns})\epsilon_{ij} \tag{15}$$

$$m_{ij} = 2\mu(z_{ns})[l(z_{ns})]^2 X_{ij} \tag{16}$$

where δ_{ij} is the Kronecker symbol, l is the material length scale parameter which reflects the effect of couple stress. Also, the Láme's constants can be defined by

$$\lambda(z_{ns}) = \frac{E(z_{ns})\nu(z_{ns})}{[1+\nu(z_{ns})][1-2\nu(z_{ns})]} \tag{17}$$

$$\mu(z_{ns}) = \frac{E(z_{ns})}{2[1+\nu(z_{ns})]} \tag{18}$$

4. The refined FGM beam model

By defining exact location of neutral surface, the displacement components based on axial u, bending w_b and shear w_s displacements may be introduced as

$$u_x(x, z_{ns}, t) = u_0(x,t) - z_{ns}\frac{\partial w_b}{\partial x} - f(z_{ns})\frac{\partial w_s}{\partial x} \tag{19}$$

$$u_y(x, z_{ns}, t) = 0 \tag{20}$$

$$u_z(x, z_{ns}, t) = w_b(x,t) + w_s(x,t) \tag{21}$$

Also:

- According to classical beam theory (CBT):

$$w_s(x,t) = 0 \tag{22}$$

- According to first order beam theory (FBT):

$$f(z_{ns}) = 0 \tag{23}$$

- According to sinusoidal beam theory (SBT):

$$f(z_{ns}) = (z_{ns} + C) - \frac{h}{\pi}\sin\left(\frac{\pi(z_{ns}+C)}{h}\right) \tag{24}$$

- According to third-order beam theory (TBT):

$$f(z_{ns}) = -\frac{z_{ns}+C}{4} + \frac{5(z_{ns}+C)^3}{3h^2} \tag{25}$$

Next, the strains based on the modified beam model have been obtained as

$$\epsilon_x = \frac{\partial u_0}{\partial x} - z_{ns}\frac{\partial^2 w_b}{\partial x^2} - f(z_{ns})\frac{\partial^2 w_s}{\partial x^2} \tag{26}$$

$$\epsilon_y = \epsilon_z = \gamma_{xy} = \gamma_{yz} = 0 \tag{27}$$

$$\gamma_{xz} = 2\epsilon_{xz} = g(z_{ns})\frac{\partial w_s}{\partial x} \tag{28}$$

where $g(z_{ns}) = 1 - f'(z_{ns})$. In addition, Eqs. (12), (13) and (14) give

$$\begin{aligned} \theta_y &= -\frac{\partial w_b}{\partial x} - \frac{1}{2}\psi(z_{ns})\frac{\partial w_s}{\partial x} \\ \theta_x &= \theta_z = 0 \end{aligned} \tag{29}$$

with $\psi(z_{ns}) = 1 + f'(z_{ns})$. Substitution of Eq. (29) into (13) leads to the following expression for the non-zero components of the symmetric curvature tensor

$$\begin{aligned} X_{xy} &= -\frac{1}{2}\frac{\partial^2 w_b}{\partial x^2} - \frac{1}{4}\psi(z_{ns})\frac{\partial^2 w_s}{\partial x^2} \\ X_{yz} &= -\frac{1}{4}f''(z_{ns})\frac{\partial w_s}{\partial x} \end{aligned} \tag{30}$$

$$X_{xx} = X_{yy} = X_{zz} = X_{xz} = 0 \tag{31}$$

5. The governing equations

Next, one might express the Hamilton's rule as follows based on strain energy (U) and kinetic energy (K)

$$\int_0^T \delta(U+V-K)dt = 0 \tag{32}$$

and V is the work of non-conservative loads. Based on above relation we have

$$\begin{aligned}\delta U &= \int_0^L \int_{-\frac{h}{2}-C}^{\frac{h}{2}-C} \left(\sigma_{ij}\delta\epsilon_{ij} + m_{ij}\delta X_{ij}\right) dz_{ns}dx \\ &= \int_0^L \int_{-\frac{h}{2}-C}^{\frac{h}{2}-C} \left(\sigma_x\delta\epsilon_x + \tau_{xz}\delta\gamma_{xz} + 2m\delta X_{xy} \right. \\ &\qquad \left. +2m_{yz}\delta X_{yz}\right) dZ_{ns}dx \\ &= \int_0^L \left(N\frac{d\delta u_0}{dx} - (M_b + Y_1)\frac{d^2\delta w_b}{dx^2} \right. \\ &\quad -\left(M_s + \frac{1}{2}Y_1 + \frac{1}{2}Y_2\right)\frac{d^2\delta w_s}{dx^2} \\ &\quad \left. +\left(Q - \frac{1}{2}Y_3\right)\frac{d\delta w_s}{dx}\right) dx\end{aligned} \tag{33}$$

in which

$$\begin{aligned}(N, M_b, M_s) &= \int_{-\frac{h}{2}-C}^{\frac{h}{2}-C} (1, z_{ns}, f)\sigma_x dz_{ns} \\ Q &= \int_{-\frac{h}{2}-C}^{\frac{h}{2}-C} g\tau_{xz}dz_{ns}\end{aligned} \tag{34}$$

$$\begin{aligned}(Y_1, Y_2) &= \int_{-\frac{h}{2}-C}^{\frac{h}{2}-C} (1, f')m_{xy}dz_{ns} \\ Y_3 &= \int_{-\frac{h}{2}-C}^{\frac{h}{2}-C} f''m_{yz}dz_{ns}\end{aligned} \tag{35}$$

The variation for the work of non-conservative force is expressed by

$$\delta V = -\int_0^L N^T \frac{\partial(w_b + w_s)}{\partial x}\delta\left(\frac{\partial(w_b + w_s)}{\partial x}\right)dx \tag{36}$$

Herein, N^T defines thermal loading and may be defined by

$$\begin{aligned}N^T = \int_{-\frac{h}{2}-C}^{\frac{h}{2}-C} &\lambda(z_{ns}, T)\frac{1-\nu(z_{ns}, T)}{\nu(z_{ns}, T)} \\ &\gamma(z_{ns}, T)(T - T_0)dz\end{aligned} \tag{37}$$

in such a way that T_0 is a specific temperature and $T = \Delta T + T_0$. Also, the kinetic energy is obtained as

$$\begin{aligned}K = \frac{1}{2}\int_0^L \int_A \rho(z_{ns}, T)\left(\left(\frac{\partial u_x}{\partial t}\right)^2 + \left(\frac{\partial u_y}{\partial t}\right)^2 \right. \\ \left. + \left(\frac{\partial u_z}{\partial t}\right)^2\right) dAdx\end{aligned} \tag{38}$$

And its variation becomes

$$\begin{aligned}\delta K &= \int_0^L \int_{-\frac{h}{2}-C}^{\frac{h}{2}-C} \rho(z_{ns}, T)\left[\dot{u}_x\delta\dot{u}_x + \dot{u}_y\delta\dot{u}_y\right] dz_{ns}dx \\ &= \int_0^L \{I_0[\dot{u}_0\delta\dot{u}_0 + (\dot{w}_b + \dot{w}_s)(\delta\dot{w}_b + \delta\dot{w}_s)] \\ &\quad -I_1\left(\dot{u}_0\frac{d\delta\dot{w}_b}{dx} + \frac{d\dot{w}_b}{dx}\delta\dot{u}_0\right) + I_2\left(\frac{d\dot{w}_b}{dx}\frac{d\delta\dot{w}_b}{dx}\right) \\ &\quad -J_1\left(\dot{u}_0\frac{d\delta\dot{w}_s}{dx} + \frac{d\dot{w}_s}{dx}\delta\dot{u}_0\right) + K_2\left(\frac{d\dot{w}_s}{dx}\frac{d\delta\dot{w}_s}{dx}\right) \\ &\quad +J_2\left(\frac{d\dot{w}_b}{dx}\frac{d\delta\dot{w}_s}{dx} + \frac{d\dot{w}_s}{dx}\frac{d\delta\dot{w}_b}{dx}\right)\}dx\end{aligned} \tag{39}$$

where

$$\begin{aligned}&(I_0, I_1, J_1, I_2, J_2, K_2) \\ &= \int_{-\frac{h}{2}-C}^{\frac{h}{2}-C} (1, z_{ns}, f, {z_{ns}}^2, z_{ns}f, f^2)\rho(z_{ns})dz_{ns}\end{aligned} \tag{40}$$

Substituting Eqs. (33)-(39) into Eq. (32) then collecting the coefficients for field variables results in three equations of motion

$$\delta u_0 : \frac{dN}{dx} = I_0\ddot{u}_0 - I_1\frac{d\ddot{w}_b}{dx} - J_1\frac{d\ddot{w}_s}{dx} \tag{41}$$

$$\begin{aligned}\delta w_b : \frac{d^2M_b}{dx^2} + \frac{d^2Y_1}{dx^2} - N^T\frac{d^2(w_b+w_s)}{dx^2} \\ = I_0(\ddot{w}_b + \ddot{w}_s) + I_1\frac{d\ddot{u}_0}{dx} - I_2\frac{d^2\ddot{w}_b}{dx^2} - J_2\frac{d^2\ddot{w}_s}{dx^2}\end{aligned} \tag{42}$$

$$\begin{aligned}\delta w_s : \frac{d^2M_s}{dx^2} + \frac{1}{2}\frac{d^2Y_1}{dx^2} + \frac{1}{2}\frac{d^2Y_2}{dx^2} - \frac{1}{2}\frac{dY_3}{dx} + \frac{dQ}{dx} \\ -N^T\frac{d^2(w_b+w_s)}{dx^2} = I_0(\ddot{w}_b + \ddot{w}_s) \\ +J_1\frac{d\ddot{u}_0}{dx} - J_2\frac{d^2\ddot{w}_b}{dx^2} - K_2\frac{d^2\ddot{w}_s}{dx^2}\end{aligned} \tag{43}$$

Next, all edge conditions for $x = 0, L$ may be expressed by

$$\begin{matrix}\text{Specify} \\ u_o \quad or \quad N\end{matrix} \tag{44}$$

$$\begin{matrix}\text{Specify} \\ w_b \text{ or } V_b = \frac{dM_b}{dx} + \frac{dY_1}{dx} - I_1\ddot{u}_0 + I_2\frac{d\ddot{w}_b}{dx}\end{matrix} \tag{45}$$

$$+J_2\frac{d\ddot{w}_s}{dx}-N^T\frac{d(w_b+w_s)}{dx} \tag{45}$$

Specify

$$w_s \text{ or } V_s=\frac{dM_s}{dx}+\frac{1}{2}\frac{dY_1}{dx}+\frac{1}{2}\frac{dY_2}{dx}-\frac{1}{2}Y_3+Q-J_1\ddot{u}_0 +J_2\frac{d\ddot{w}_b}{dx}+K_2\frac{d\ddot{w}_s}{dx}-N^T\frac{d(w_b+w_s)}{dx} \tag{46}$$

$$\text{Specify}\quad \frac{dw_b}{dx}\quad \text{or}\quad M_b+Y_1-N^T \tag{47}$$

$$\text{Specify}\quad \frac{dw_s}{dx}\quad \text{or}\quad M_s+\frac{1}{2}Y_1+\frac{1}{2}Y_2-N^T \tag{48}$$

Three equations of motion based on neutral surface location and microbeam assumptions will be achieved by placing Eqs. (34)-(35) in Eqs. (41)-(43) by

$$A_{11}\frac{d^2u_0}{dx^2}-B_{11}\frac{d^3w_b}{dx^3}-B_{11}^s\frac{d^3w_s}{dx^3} =I_0\ddot{u}_0-I_1\frac{d\ddot{w}_b}{dx}-J_1\frac{d\ddot{w}_s}{dx} \tag{49}$$

$$-(D_{11}+A_{13})\frac{d^4w_b}{dx^4}+B_{11}\frac{d^3u_0}{dx^3} -\left(D_{11}^s+\frac{1}{2}(A_{13}+B_{13})\right)\frac{d^4w_s}{dx^4}-N^T\frac{d^2(w_b+w_s)}{dx^2} =I_0(\ddot{w}_b+\ddot{w}_s)+I_1\frac{d\ddot{u}_0}{dx}-I_2\frac{d^2\ddot{w}_b}{dx^2}-J_2\frac{d^2\ddot{w}_s}{dx^2} \tag{50}$$

$$B_{11}^s\frac{d^3u_0}{dx^3}-\left(D_{11}^s+\frac{1}{2}(A_{13}+B_{13})\right)\frac{d^4w_b}{dx^4} -\left(H_{11}^s+\frac{1}{4}(A_{13}+2B_{13}+D_{13})\right)\frac{d^4w_s}{dx^4} +\left(A_{55}^s+\frac{1}{4}E_{13}\right)\frac{d^2w_s}{dx^2}-N^T\frac{d^2(w_b+w_s)}{dx^2} =I_0(\ddot{w}_b+\ddot{w}_s)+J_1\frac{d\ddot{u}_0}{dx}-J_2\frac{d^2\ddot{w}_b}{dx^2}-K_2\frac{d^2\ddot{w}_s}{dx^2} \tag{51}$$

so that A_{11}, B_{11}^s, etc., define the microbeam stiffness, introduced by

$$(A_{11},B_{11},D_{11},B_{11}^s,D_{11}^s,H_{11}^s) =\int_{-\frac{h}{2}-C}^{\frac{h}{2}-C}\lambda(z_{ns})\frac{1-\nu(Z_{ns})}{\nu(Z_{ns})}(1,z,z_{ns}^2,f,z_{ns}f,f^2)dz_{ns} \tag{52}$$

$$(A_{13},B_{13},D_{13},E_{13}) =\int_{-\frac{h}{2}-C}^{\frac{h}{2}-C}\mu(z_{ns})[l(z_{ns})]^2[1,f',(f')^2,(f'')^2]dz_{ns} \tag{53}$$

$$A_{55}^s=\int_{-\frac{h}{2}-C}^{\frac{h}{2}-C}\mu(z_{ns})g^2dz_{ns} \tag{54}$$

6. Solution by differential quadrature method (DQM)

In the present chapter, differential quadrature method (DQM) has been utilized for solving the governing equations for microbeam. According to DQM, at an assumed grid point (x_i,y_j) the derivatives for function F are supposed as weighted linear summation of all functional values within the computation domains as

$$\frac{d^nF}{dx^n}\Big|_{x=x_i}=\sum_{j=1}^{N}C_{ij}^{(n)}F(x_j) \tag{55}$$

where

$$C_{ij}^{(1)}=\frac{\pi(x_i)}{(x_i-x_j)\,\pi(x_j)} \qquad i,j=1,2,\dots,N,\quad i\neq j \tag{56}$$

in which $\pi(x_i)$ is defined by

$$\pi(x_i)=\prod_{j=1}^{N}(x_i-x_j),\quad i\neq j \tag{57}$$

And when $i=j$

$$C_{ij}^{(1)}=C_{ii}^{(1)}=-\sum_{k=1}^{N}C_{ik}^{(1)}, \qquad i=1,2,\dots,N,\quad i\neq k,\quad i=j \tag{58}$$

Then, weighting coefficients for high orders derivatives may be expressed by

$$C_{ij}^{(2)}=\sum_{k=1}^{N}C_{ik}^{(1)}C_{kj}^{(1)}$$
$$C_{ij}^{(3)}=\sum_{k=1}^{N}C_{ik}^{(1)}C_{kj}^{(2)}=\sum_{k=1}^{N}C_{ik}^{(2)}C_{kj}^{(1)}$$
$$C_{ij}^{(4)}=\sum_{k=1}^{N}C_{ik}^{(1)}C_{kj}^{(3)}=\sum_{k=1}^{N}C_{ik}^{(3)}C_{kj}^{(1)}$$
$$i,j=1,2,\dots,N. \tag{59}$$

According to presented approach, the dispersions of grid points based upon Gauss-Chebyshev-Lobatto assumption are expressed as

$$x_i=\frac{a}{2}\left[1-\cos\left(\frac{i-1}{N-1}\pi\right)\right]\quad i=1,2,\dots,N, \tag{60}$$

Next, the time derivative for displacement components may be determined by

$$u(x,t)=U(x)e^{i\omega t} \tag{61}$$

$$w_b(x,t)=W_b(x)e^{i\omega t} \tag{62}$$

$$w_s(x,t)=W_s(x)e^{i\omega t} \tag{63}$$

where *U* and *W* denote vibration amplitudes and ω defines the vibrational frequency. Then, it is possible to express

obtained boundary conditions as:

- Simply supported- simply supported (S-S):

$$w_b = w_s = 0, N_{xx} = 0, M_{xx}^b = 0 \quad \text{at} \quad x = 0, L \tag{64}$$

- Clamped-clamped (C-C):

$$w_b = w_s = 0, \quad \frac{\partial w_b}{\partial x} = \frac{\partial w_s}{\partial x} = 0 \quad \text{at} \quad x = 0, L \tag{65}$$

Now, one can express the modified weighting coefficients for all edges simply-supported as

$$\begin{aligned} \bar{C}_{1,j}^{(2)} &= \bar{C}_{N,j}^{(2)} = 0, \quad i = 1, 2, \dots, M, \\ \bar{C}_{i,1}^{(2)} &= \bar{C}_{1,M}^{(2)} = 0, \quad i = 1, 2, \dots, N. \end{aligned} \tag{66}$$

and

$$\bar{C}_{ij}^{(3)} = \sum_{k=1}^{N} C_{ik}^{(1)} \bar{C}_{kj}^{(2)} \qquad \bar{C}_{ij}^{(4)} = \sum_{k=1}^{N} C_{ik}^{(1)} \bar{C}_{kj}^{(3)} \tag{67}$$

By placing Eqs. (61)-(63) into Eqs. (49)-(51) and performing some simplifications for collecting the coefficients of displacements (U, W_b, W_s) leads to the following system based on mass matrix[M] and stiffness matrix [K] as

$$\{[K] + \omega^2[M]\} \begin{Bmatrix} U \\ W_b \\ W_s \end{Bmatrix} = 0 \tag{68}$$

where the components of [K] and [M] are

$$\begin{aligned} K_{11} &= \sum_{j=1}^{N} \left(A_{11} C_{ij}^{(2)}\right), \quad K_{12} = \sum_{j=1}^{N} \left(B_{11} C_{ij}^{(3)}\right) \\ K_{13} &= \sum_{j=1}^{N} \left(B_{11}^s C_{ij}^{(3)}\right), \quad K_{21} = \sum_{j=1}^{N} \left(-B_{11} C_{ij}^{(3)}\right) \\ K_{22} &= \sum_{j=1}^{N} \left(-(D_{11} + A_{13}) C_{ij}^{(4)} - N^T C_{ij}^{(2)}\right) \\ K_{23} &= K_{32} \\ &= \sum_{j=1}^{N} \left(-\left(D_{11}^s + \frac{1}{2}(A_{13} + B_{13})\right) C_{ij}^{(4)} - N^T C_{ij}^{(2)}\right) \\ K_{31} &= \sum_{j=1}^{N} \left(-B_{11}^s C_{ij}^{(3)}\right) \\ K_{33} &= \sum_{j=1}^{N} \left(-\left(H_{11}^s + \frac{1}{4}(A_{13} + 2B_{13} + D_{13})\right) C_{ij}^{(4)} \right. \\ &\quad \left. -\left(N^T - A_{55}^s + \frac{1}{4} E_{13}\right) C_{ij}^{(2)}\right) \end{aligned} \tag{69}$$

$$M_{11} = \sum_{j=1}^{N} (I_0 C_{ij}^{(0)}), \quad M_{12} = \sum_{j=1}^{N} (I_1 C_{ij}^{(1)}) \tag{70}$$

$$\begin{aligned} M_{13} &= \sum_{j=1}^{N} (J_1 C_{ij}^{(3)}), \quad M_{21} = \sum_{j=1}^{N} (-I_1 C_{ij}^{(1)}) \\ M_{22} &= \sum_{j=1}^{N} (I_0 C_{ij}^{(0)} - I_2 C_{ij}^{(2)}) \\ M_{23} &= M_{32} = \sum_{j=1}^{N} (I_0 C_{ij}^{(0)} - J_2 C_{ij}^{(2)}) \\ M_{31} &= \sum_{j=1}^{N} (-J_1 C_{ij}^{(1)}), \quad M_{33} = \sum_{j=1}^{N} (I_0 C_{ij}^{(0)} - K_2 C_{ij}^{(2)}) \end{aligned} \tag{70}$$

7. Numerical results and discussions

The presented research examines vibration behaviors of thermally loaded porous FG micro-dimension beams based on refined beam model and DQ method. Modified couple stress coefficient is used in order to define the size-dependent behavior of micro-size beam. Presented results indicate the prominence of temperature variation, material gradient index, couple stress coefficient, and porosities on vibrational frequencies of FG micro-size beam. A verification study is presented in Table 2 for FG microbeam with comparing the vibrational frequency presented by DQM and those obtained by Al-Basyouni *et al*. (2015) based on diverse beam theories. The following relation is accomplished in order to compute the non-dimensional natural frequencies

$$\bar{\omega} = \frac{\omega L^2}{h} \sqrt{\frac{\rho_c}{E_c}} \tag{71}$$

In Fig. 2, the variation of normalized frequencies of an FG micro-dimension beam versus power-law exponent (p) is represented for several porosity coefficients when L/h = 20. By selecting α = 0, the vibrational frequencies based upon classic and perfect beam assumption will be derived. Actually, selecting p = 0 gives the frequency in the context of isotropic material modeling and discarding inhomogeneity impacts. It can be understood from Fig. 2 that vibration frequency of system may decline or rise with porosity coefficient and will reduce with material index (p). This observation is valid for all values of porosity coefficient. So, vibration behavior of the microbeam system is dependent on porosity effects.

Figs. 3 and 4 indicate the impact of pore parameter on vibration frequency curves of porosity-dependent micro-sized beams when L = 30h based on even pore dispersion. Different amounts of pore parameter have been selected (α = 0, 0.1 and 0.2). The result based on α = 0 is related to perfect micro-size beams. For both porous and perfect micro-size beams, the zero value of vibration frequency denotes the thermal buckling. One can find that the vibration frequencies become smaller by increasing in temperature value highlighting the intrinsic softening influence related to thermal loading. Then, one can find that increasing in pore parameter yields a lower vibration frequency at small values of temperature rise. The reason

Table 2 Verification of the non-dimension natural frequency for a S–S FG micro-beam with various gradient exponents at $h/l = 2$

L/h	Beam theory		Gradient index			
			p = 0.3	p = 1	p = 3	p = 10
10	Al-Basyouni *et al.* (2015)	Classic theory	7.9307	6.6159	5.7362	5.1231
		First order theory	7.8233	6.5211	5.6383	5.0237
		Sinusoidal theory	7.8722	6.5670	5.6876	5.0731
	Present		7.8721	6.5667	5.6877	5.0717
100	Al-Basyouni *et al.* (2015)	Classic theory	7.9651	6.6471	5.7633	5.1453
		First order theory	7.9640	6.6461	5.7623	5.1442
		Sinusoidal theory	7.9645	6.6466	5.7628	5.1448
	Present		7.9642	6.6467	5.7629	5.1451

comes from the reduction of micro-sized beams stiffness with the incorporation of porosities. However, at larger values of temperature rise, both porosity and thermal loading have notable influences on structural stiffness of the microbeam.

In Fig. 5, the variation of normalized frequencies of an FG micro-dimension beam versus porosity factor is represented for several couple stress (h/l) coefficients when L/h = 20 and p = 1. By selecting h/l = 0, the vibrational

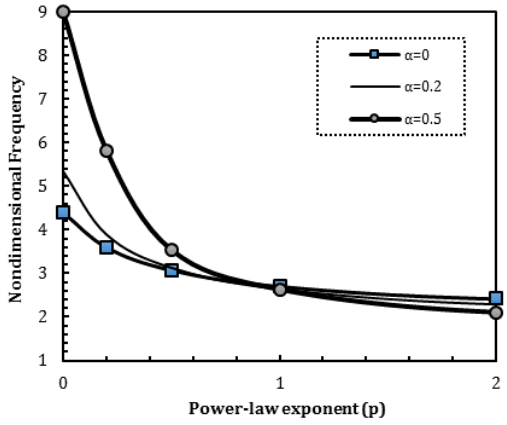

Fig. 2 Changing of non-dimension frequency of S-S FG microbeam against material index and porosity ($L/h = 20, h/l = 2$)

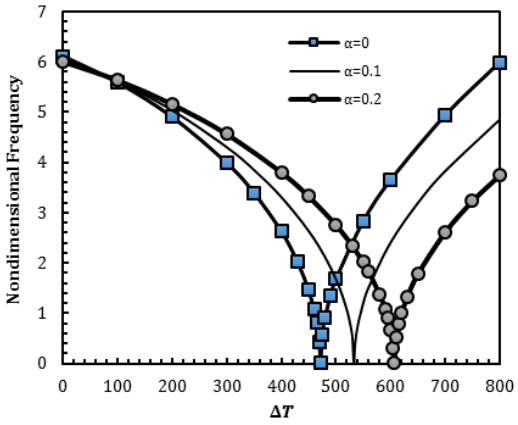

Fig. 4 Changing of non-dimension frequency of C-C porous FG microbeam against temperature change based on diverse values of porosity factor ($L/h = 30,\ h/l = 2,\ p = 1$)

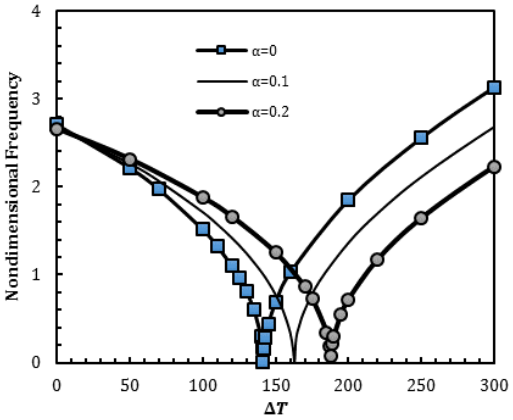

Fig. 3 Changing of non-dimension frequency of S–S porous FG microbeam against temperature change based on diverse values of porosity factor ($L/h = 30,\ h/l = 2,\ p = 1$)

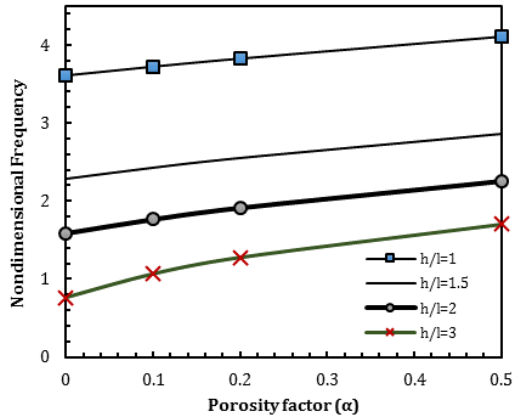

Fig. 5 Changing of non-dimension frequency of S-S FG porous microbeam against porosity factor based on diverse couple stress parameters (ΔT = 200, L/h = 20, $p = 1$)

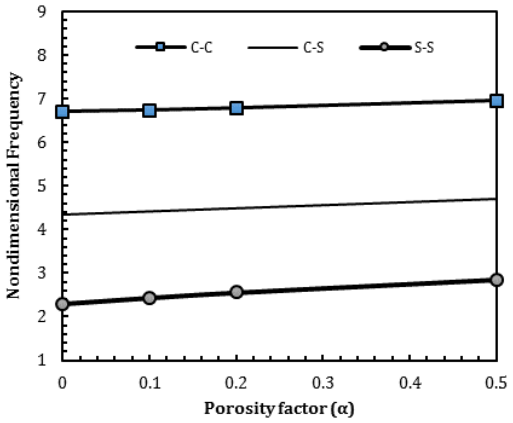

Fig. 6 Changing of non-dimension frequency of S-S porous FG microbeam against porosity factor based on diverse edge conditions (ΔT = 200, L/h = 20, $p = 1$)

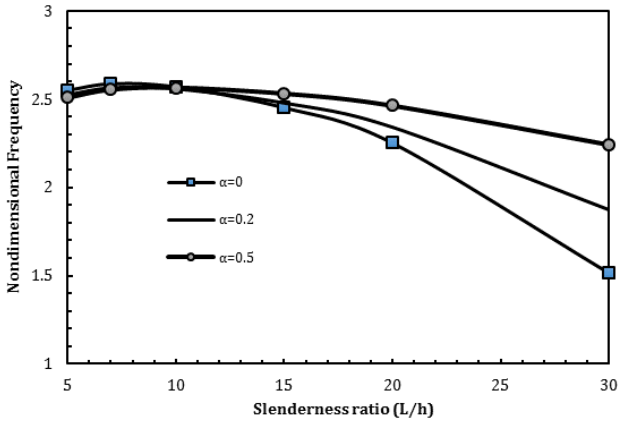

Fig. 7 Changing of non-dimension frequency of S-S porous FG microbeam against slenderness ratio based on diverse porosity factors (ΔT = 100, $h/l = 2$, $p = 1$)

frequencies based upon classic beam assumption will be derived. Actually, selecting h/l = 0 gives the frequency macro scale beams with discarding couple stress impacts. It can be understood from Fig. 5 that vibration frequency of system will change with couple stress coefficient. This observation is valid for all values of pore factor. So, vibration behavior of the microbeam system is dependent on scale effects. Another finding is that increasing of pore factor is corresponding to higher ratio of structural stiffness to mass density of the micro-dimension beam as well as larger vibration frequency.

The impact of pore factor and boundary conditions on non-dimension frequency of an FG microbeam subjected to uniform temperature changes at ΔT = 200, L/h = 20, $h/l = 2$, $p = 1$ has been illustrated in Fig. 6. According to our findings, increase of the number of constraints at edges makes the micro-size beam stiffer and vibrational frequency increases. Furthermore, at a prescribed temperature value and pore factor, the results for porous FG micro-size beam follows this relation: C-C > C-S > S-S. Accordingly, vibrational behaviors of porous FG micro-size beams depend on the kind of edge condition.

In Fig. 7, the variation of the dimensionless frequency of S-S FG porous microbeam with respect to slenderness ratio according to different porosity volume fractions is shown at ΔT = 100, $h/l = 2$, $p = 1$. It can be understood that dimensionless frequency decreases when slenderness ratio increases at a prescribed porosity volume fraction. So, thinner porous FG microbeams have lower frequencies compared to thicker one. Moreover, effect of porosity volume fraction on vibration frequencies becomes more significant at larger slenderness ratios.

8. Conclusions

Presented research examined vibration behaviors of thermally loaded porous FG micro-size beams based on three-variable beam model and DQ method. Modified couple stress coefficient was used in order to define the size-dependent behavior of micro-size beam. It was seen that vibration frequency raised with couple stress coefficient. Another finding was that increasing of temperature or in-plane mechanical load was corresponding to lower structural stiffness of the micro-dimension beam as well as smaller vibration frequency. Also, increase of porosity factor may reduce the value of vibrational frequency. It was stated that increasing in temperature diminished the structural stiffness and vibrational frequencies decreased until a critical temperature in which frequency magnitude became zero.

Acknowledgments

The authors would like to thank Mustansiriyah university (www.uomustansiriyah.edu.iq) Baghdad-Iraq for its support in the present work.

References

Ahmed, R.A., Fenjan, R.M. and Faleh, N.M. (2019), "Analyzing post-buckling behavior of continuously graded FG nanobeams with geometrical imperfections", *Geomech. Eng., Int. J.*, **17**(2), 175-180. https://doi.org/10.12989/gae.2019.17.2.175

Akgöz, B. and Civalek, Ö. (2014), "Thermo-mechanical buckling behavior of functionally graded microbeams embedded in elastic medium", *Int. J. Eng. Sci.*, **85**, 90-104. https://doi.org/10.1016/j.ijengsci.2014.08.011

Al-Basyouni, K.S., Tounsi, A. and Mahmoud, S.R. (2015), "Size dependent bending and vibration analysis of functionally graded micro beams based on modified couple stress theory and neutral surface position", *Compos. Struct.*, **125**, 621-630. https://doi.org/10.1016/j.compstruct.2014.12.070

Attia, M.A. and Rahman, A.A.A. (2018), "On vibrations of functionally graded viscoelastic nanobeams with surface effects", *Int. J. Eng. Sci.*, **127**, 1-32. https://doi.org/10.1016/j.ijengsci.2018.02.005

Ayache, B., Bennai, R., Fahsi, B., Fourn, H., Atmane, H.A. and Tounsi, A. (2018), "Analysis of wave propagation and free vibration of functionally graded porous material beam with a novel four variable refined theory", *Earthq. Struct., Int. J.*, **15**(4), 369-382. https://doi.org/10.12989/eas.2018.15.4.369

Barretta, R., Čanađija, M., Luciano, R. and de Sciarra, F.M.

(2018), "Stress-driven modeling of nonlocal thermoelastic behavior of nanobeams", *Int. J. Eng. Sci.*, **126**, 53-67. https://doi.org/10.1016/j.ijengsci.2018.02.012

Belabed, Z., Bousahla, A.A., Houari, M.S.A., Tounsi, A. and Mahmoud, S.R. (2018), "A new 3-unknown hyperbolic shear deformation theory for vibration of functionally graded sandwich plate", *Earthq. Struct.*, *Int. J.*, **14**(2), 103-115. https://doi.org/10.12989/eas.2018.14.2.103

Benadouda, M., Atmane, H.A., Tounsi, A., Bernard, F. and Mahmoud, S.R. (2017), "An efficient shear deformation theory for wave propagation in functionally graded material beams with porosities", *Earthq. Struct.*, *Int. J.*, **13**(3), 255-265. https://doi.org/10.12989/eas.2017.13.3.255

Bensattalah, T., Bouakkaz, K., Zidour, M. and Daouadji, T.H. (2019), "Critical buckling loads of carbon nanotube embedded in Kerr's medium", *Adv. Nano Res., Int. J.*, **6**(4), 339-356. https://doi.org/10.12989/anr.2018.6.4.339

Besseghier, A., Heireche, H., Bousahla, A.A., Tounsi, A. and Benzair, A. (2015), "Nonlinear vibration properties of a zigzag single-walled carbon nanotube embedded in a polymer matrix", *Adv. Nano Res., Int. J.*, **3**(1), 29-37. https://doi.org/10.12989/anr.2015.3.1.029

Castrucci, P. (2014), "Carbon nanotube/silicon hybrid heterojunctions for photovoltaic devices", *Adv. Nano Res., Int. J.*, **2**(1), 23-56. https://doi.org/10.12989/anr.2014.2.1.023

Chemi, A., Heireche, H., Zidour, M., Rakrak, K. and Bousahla, A.A. (2015)", Critical buckling load of chiral double-walled carbon nanotube using non-local theory elasticity", *Adv. Nano Res., Int. J.*, **3**(4), 193-206. https://doi.org/10.12989/anr.2015.3.4.193

Civalek, Ö. and Demir, Ç. (2016), "A simple mathematical model of microtubules surrounded by an elastic matrix by nonlocal finite element method", *Appl. Mathe. Computat.*, **289**, 335-352. https://doi.org/10.1016/j.amc.2016.05.034

Fernández-Sáez, J., Zaera, R., Loya, J.A. and Reddy, J.N. (2016), "Bending of Euler–Bernoulli beams using Eringen's integral formulation: a paradox resolved", *Int. J. Eng. Sci.*, **99**, 107-116. https://doi.org/10.1016/j.ijengsci.2015.10.013

Hadji, L., Daouadji, T.H. and Bedia, E.A. (2016), "Dynamic behavior of FGM beam using a new first shear deformation theory", *Earthq. Struct., Int. J.*, **10**(2), 451-461. https://doi.org/10.12989/eas.2016.10.2.451

Ke, L.L., Wang, Y.S., Yang, J. and Kitipornchai, S. (2012), "Nonlinear free vibration of size-dependent functionally graded microbeams", *Int. J. Eng. Sci.*, **50**(1), 256-267. https://doi.org/10.1016/j.ijengsci.2010.12.008

Kiani, Y. and Eslami, M.R. (2013), "An exact solution for thermal buckling of annular FGM plates on an elastic medium", *Compos. Part B: Eng.*, **45**(1), 101-110. https://doi.org/10.1016/j.compositesb.2012.09.034

Liu, C., Ke, L.L., Wang, Y.S., Yang, J. and Kitipornchai, S. (2013), "Thermo-electro-mechanical vibration of piezoelectric nanoplates based on the nonlocal theory", *Compos. Struct.*, **106**, 167-174. https://doi.org/10.1016/j.compstruct.2013.05.031

Lü, C.F., Lim, C.W. and Chen, W.Q. (2009), "Size-dependent elastic behavior of FGM ultra-thin films based on generalized refined theory", *Int. J. Solids Struct.*, **46**(5), 1176-1185. https://doi.org/10.1016/j.ijsolstr.2008.10.012

Mahesh, V. and Kattimani, S. (2019), "Finite element simulation of controlled frequency response of skew multiphase magneto-electro-elastic plates", *J. Intel. Mater. Syst. Struct.*, **30**(12), 1757-1771. https://doi.org/10.1177/1045389X19843674

Mahesh, V., Sagar, P.J. and Kattimani, S. (2018), "Influence of coupled fields on free vibration and static behavior of functionally graded magneto-electro-thermo-elastic plate", *J. Intel. Mater. Syst. Struct.*, **29**(7), 1430-1455. https://doi.org/10.1177/1045389X17740739

Mahesh, V., Kattimani, S., Harursampath, D. and Trung, N.T. (2019), "Coupled evaluation of the free vibration characteristics of magneto-electro-elastic skew plates in hygrothermal environment", *Smart Struct. Syst., Int. J.*, **24**(2), 267-292. https://doi.org/10.12989/sss.2019.24.2.267

Mahmoudi, A., Benyoucef, S., Tounsi, A., Benachour, A. and Bedia, E.A.A. (2018), "On the effect of the micromechanical models on the free vibration of rectangular FGM plate resting on elastic foundation", *Earthq. Struct., Int. J.*, **14**(2), 117-128. https://doi.org/10.12989/eas.2018.14.2.117

Safa, A., Hadji, L., Bourada, M. and Zouatnia, N. (2019), "Thermal vibration analysis of FGM beams using an efficient shear deformation beam theory", *Earthq. Struct., Int. J.*, **17**(3), 329-336. https://doi.org/10.12989/eas.2019.17.3.329

She, G.L., Yan, K.M., Zhang, Y.L., Liu, H.B. and Ren, Y.R. (2018), "Wave propagation of functionally graded porous nanobeams based on non-local strain gradient theory", *Eur. Phys. J. Plus*, **133**(9), 368. https://doi.org/10.1140/epjp/i2018-12196-5

She, G.L., Jiang, X.Y. and Karami, B. (2019), "On thermal snap-buckling of FG curved nanobeams", *Mater. Res. Express*, **6**, 115008. https://doi.org/10.1088/2053-1591/ab44f1

Şimşek, M. and Kocatürk, T. (2009), "Free and forced vibration of a functionally graded beam subjected to a concentrated moving harmonic load", *Compos. Struct.*, **90**(4), 465-473. https://doi.org/10.1016/j.compstruct.2009.04.024

Şimşek, M. and Reddy, J.N. (2013), "Bending and vibration of functionally graded microbeams using a new higher order beam theory and the modified couple stress theory", *Int. J. Eng. Sci*, **64**, 37-53. https://doi.org/10.1016/j.ijengsci.2012.12.002

Tounsi, A., Benguediab, S., Adda, B., Semmah, A. and Zidour, M. (2013), "Nonlocal effects on thermal buckling properties of double-walled carbon nanotubes", *Adv. Nano Res., Int. J.*, **1**(1), 1-11. https://doi.org/10.12989/anr.2013.1.1.001

Vinyas, M. (2020a), "Computational Analysis of Smart Magneto-Electro-Elastic Materials and Structures: Review and Classification", *Arch. Computat. Methods Eng.*, 1-44. https://doi.org/10.1007/s11831-020-09406-4

Vinyas, M. (2020b), "On frequency response of porous functionally graded magneto-electro-elastic circular and annular plates with different electro-magnetic conditions using HSDT", *Compos. Struct.*, **240**, 112044. https://doi.org/10.1016/j.compstruct.2020.112044

Vinyas, M. (2020c), "Interphase effect on the controlled frequency response of three-phase smart magneto-electro-elastic plates embedded with active constrained layer damping: FE study", *Mater. Res. Express*, **6**(12), 125707. https://doi.org/10.1088/2053-1591/ab6649

Vinyas, M. and Kattimani, S.C. (2017a), "A finite element based assessment of static behavior of multiphase magneto-electro-elastic beams under different thermal loading", *Struct. Eng. Mech., Int. J.*, **62**(5), 519-535. https://doi.org/10.12989/sem.2017.62.5.519

Vinyas, M. and Kattimani, S.C. (2017b), "Static analysis of stepped functionally graded magneto-electro-elastic plates in thermal environment: a finite element study", *Compos. Struct.*, **178**, 63-86. https://doi.org/10.1016/j.compstruct.2017.06.068

Vinyas, M. and Kattimani, S.C. (2017c), "Hygrothermal analysis of magneto-electro-elastic plate using 3D finite element analysis", *Compos. Struct.*, **180**, 617-637. https://doi.org/10.1016/j.compstruct.2017.08.015

Vinyas, M. and Kattimani, S.C. (2017d), "A 3D finite element static and free vibration analysis of magneto-electro-elastic beam", *Coupl. Syst. Mech., Int. J.*, **6**(4), 465-485. https://doi.org/10.12989/csm.2017.6.4.465

Vinyas, M. and Kattimani, S.C. (2018), "Investigation of the effect of BaTiO3/CoFe2O4 particle arrangement on the static response

of magneto-electro-thermo-elastic plates", *Compos. Struct.*, **185**, 51-64. https://doi.org/10.1016/j.compstruct.2017.10.073

Vinyas, M., Sandeep, A.S., Nguyen-Thoi, T., Ebrahimi, F. and Duc, D.N. (2019a), "A finite element–based assessment of free vibration behaviour of circular and annular magneto-electro-elastic plates using higher order shear deformation theory", *J. Intel. Mater. Syst. Struct.*, **30**(16), 2478-2501. https://doi.org/10.1177/1045389X19862386

Vinyas, M., Nischith, G., Loja, M.A.R., Ebrahimi, F. and Duc, N.D. (2019b), "Numerical analysis of the vibration response of skew magneto-electro-elastic plates based on the higher-order shear deformation theory", *Compos. Struct.*, **214**, 132-142. https://doi.org/10.1016/j.compstruct.2019.02.010

Vinyas, M., Harursampath, D. and Nguyen-Thoi, T. (2019c), "Influence of active constrained layer damping on the coupled vibration response of functionally graded magneto-electro-elastic plates with skewed edges", *Defence Technology*. [In press] https://doi.org/10.1016/j.dt.2019.11.016

Vinyas, M., Harursampath, D. and Thoi, T.N. (2020), "A higher order coupled frequency characteristics study of smart magneto-electro-elastic composite plates with cut-outs using finite element methods", *Defence Technol*. https://doi.org/10.1016/j.dt.2020.02.009

Wang, K.F. and Wang, B.L. (2011), "Vibration of nanoscale plates with surface energy via nonlocal elasticity", *Physica E: Low-dimens. Syst. Nanostruct.*, **44**(2), 448-453. https://doi.org/10.1016/j.physe.2011.09.019

Wattanasakulpong, N. and Ungbhakorn, V. (2014), "Linear and nonlinear vibration analysis of elastically restrained ends FGM beams with porosities", *Aerosp. Sci. Technol.*, **32**(1), 111-120. https://doi.org/10.1016/j.ast.2013.12.002

Yang, F.A.C.M., Chong, A.C.M., Lam, D.C.C. and Tong, P. (2002), "Couple stress based strain gradient theory for elasticity", *Int. J. Solids Struct.*, **39**(10), 2731-2743. https://doi.org/10.1016/S0020-7683(02)00152-X

Youcef, D.O., Kaci, A., Houari, M.S.A., Tounsi, A., Benzair, A. and Heireche, H. (2015), "On the bending and stability of nanowire using various HSDTs", *Adv. Nano Res., Int. J.*, **3**(4), 177-191. https://doi.org/10.12989/anr.2015.3.4.177

Zouatnia, N. and Hadji, L. (2019), "Effect of the micromechanical models on the bending of FGM beam using a new hyperbolic shear deformation theory", *Earthq. Struct., Int. J.*, **16**(2), 177-183. https://doi.org/10.12989/eas.2019.16.2.177

CC